Passivating a transition-metal surface for more uniform growth of graphene: Effect of Au alloying on Ni(111)

Yexin Feng, Xiaolong Yao, Zhenpeng Hu, Jing-Jun Xu, and Lixin Zhang

Phys. Rev. B **87**, 195421 — Published 13 May 2013

DOI: 10.1103/PhysRevB.87.195421

Passivating transition metal surface towards uniform growth of graphene: the mechanism study of Au-alloyed Ni (111)

Yexin Feng, Xiaolong Yao, Zhenpeng Hu, Jing-Jun Xu, and Lixin Zhang*

School of Physics, Nankai University, Tianjin 300071, P. R. China

Abstract

The atomic step edges on transition metal (TM) surface play an important role in surface catalysis due to their distinct reactivities from that of the terrace. The non-uniform growth of graphene on Ni(111) is just a such case. Using first principles calculations, we show that the step edges of Ni(111) can be passivated in varying degrees by surface alloying with a series of carefully chosen TMs. The alloyed surface can be more uniform between the edges and the terrace, able to facilitate large area and high quality growth of graphene.

PACS number(s): 81.15.Aa, 82.45.Jn, 68.65.Pq, 68.35.bd

*corresponding author, email: lxzhang@nankai.edu.cn

To grow large-area and defect free graphene sheet on transition metal (TM) surfaces using the chemical vapor deposition (CVD) technique is currently the preferred method employed in aiming at the commercial realization of the graphene-based technologies [1, 2]. Although lots of progress has been made, the qualities of the sheets are still in urgent need to be improved. The poor electric properties compared with the exfoliated graphene and the too restrictive growth conditions are the major obstacles to be overcome [3, 4].

In the experiments of the CVD growth, morphologies and defect densities of the surfaces greatly affect the crystalline quality and the electric properties of the as-grown graphene sheet [4-6]. Microscopically the atomic step edges on the surfaces are believed to play the key role concerning both the growth mode and the defect control. Both experimental and theoretical works indicated that the edges act as the favorable nucleation centers [7-9]. On the other hand, the edges are claimed to be responsible for the introduced line defects in the grown graphene sheets as well [5]. Some researchers proposed that reducing the number of the active nucleation centers like the step edges would be beneficial to the improving of the sheet quality [6, 10, 11]. Therefore, to fully understand the role of the atomic step edges in the CVD growth of graphene on the TM surfaces is crucial to the growing of large area and high quality graphene sheets for technological applications.

Many TM surfaces [Cu(111), Ni(111), Ru(0001), Ir(111), etc.] have been employed for the growth of graphene in which the surfaces act as not only substrates, but also catalysts [9, 12-22]. Among them, the Cu(111) and Ni(111) are the two most popular and promising ones but with contrasting growth properties. On the Cu(111), where the C solubility in the substrate is low, the growth of graphene is self-limiting [13] and the layer control is more accessible. However, the required growth temperature is relatively high which is close to the melting point of Cu crystal and the as-grown graphene sheets are usually polycrystalline with many domain boundaries [4, 13]. Since Ni is better in dissociating of the C precursors on surface and more lattice-matched with graphene than Cu [18, 20, 21], the required growth temperature is much lower [19]. But, due to the high C solubility in the Ni lattice, the graphene growth on the Ni(111) surface is characterized by a precipitation process in which uniform growth is very difficult to obtain and the layer control is highly challenging [16].

As reported recently by Weatherup and coworkers [17, 20], for the CVD growth of graphene on the Ni (111) surface, alloying the surface with a small quantity of Au atoms can greatly decrease the growth temperature. At the same time the crystalline quality especially the uniformity of the grown graphene sheet was obviously improved. The authors proposed that the Au atoms may decorate the high reactive surface sites, such as the step edges, and reduce the nucleation density on the surface. The effect of Au surface-alloying is very promising, and the behind mechanism could be revolutionary for the pursuing of large area and high quality grown graphene sheets on TM surfaces.

In this paper, we investigate the effect of Au alloying on the catalyzed CVD growth of graphene on the stepped Ni(111) surface. The calculations of the C adsorptions on the surface and the diffusions in the subsurface reveal that the step edges are the most favorable sites for C accumulation, highly contrasting to the terrace. Accordingly, the growth of graphene follows a highly non-uniform mode, agreeable with the experimental observations. Upon Au alloying, the Au atoms will firstly substitute the Ni atoms of the step edges rather than those of the terrace. The alloyed edges get closer to the terrace in properties of adsorbing as well as segregating C atoms, making the stepped surface more uniform between the edges and the terrace. Furthermore, the binding ability of the C atoms of the alloyed step edges can be tuned by using TMs with various numbers of d-electrons. Based on these results, a general surface passivating method is proposed for TM catalysis that could be widely applied.

Spin-polarized density-functional calculations were performed using the Vienna *ab initio* simulation package (VASP) [23]. The cutoff energy for plane wave expansion is 400eV. We use the projector augmented wave (PAW) method and the PBE exchange-correlation functional [24]. The stepped Ni(111) surface is modeled by a slab with a 10x4 surface periodic cell, containing 6 layers of Ni atoms, of which the bottom two are fixed at their optimal bulk positions. The thickness of the vacuum layer is more than 10 Å and the M-P k-point mesh is 2x4x1. The calculated lattice constant of bulk Ni is 3.53Å, agreeable with experimental value of 3.52 Å and the previous calculational results [25, 26].

The formation energies of the substitutional TM atoms (TM_{Ni}) at the Ni(111) surface are given by

$$E_f^{TM} = (E_{Alloy} - E_{Ni} - n\mu_{TM} + n\mu_{Ni})/n \qquad (1),$$

where E_{Alloy} is the total energy of the alloyed surface, E_{Ni} is the total energy of the corresponding clean Ni(111), and n is the number of Ni atoms substituted by the TM atoms. The symbols μ_{Ni} and μ_{TM} are the chemical potentials of Ni and the TM. They are calculated as in their bulk phases respectively. For a C atom, either adsorbed on the surface or dissolved in the Ni lattice, the formation energy is given by

$$E_f^{C} = E_{total} - E_{Alloy}(E_{Ni}) - \mu_C \qquad (2),$$

where E_{total} is the total energy of the surface with the C atom, $E_{Alloy}(E_{Ni})$ is the total energy of the alloyed (clean) surface as defined above, μ_C is the chemical potential of C as in graphene. The diffusion barriers of the C atoms in the Ni lattice are calculated with the nudged elastic band method [27] as implemented in the VASP code. All atoms except in the bottom two layers of the supercell are allowed to fully relax until the forces acting on the atoms are less than 0.01 eV/Å.

Based on previous experimental and theoretical reports, the growth process of graphene on Ni (111) surface can be schematically shown in Fig. 1. It is generally believed that firstly, at higher temperatures, the C atoms will dissolve into the Ni lattice after the dissociation of the precursors on the surface [16, 17, 20]. The dissolved C can then segregate out of the lattice when the temperature is decreased. The C resources are then from both the direct deposition and the segregation from the Ni lattice. On the surface the step edges may act as the nucleation centers due to the high activity. Thus C atom adsorption and segregation characteristics at the step edges are the keys for the nucleation and growth of graphene on the Ni surface. In this work, in order to reveal the effect of Au surface alloying microscopically on the graphene growth, instead of the dynamical processes of C diffusion and nucleation on the terrace of the stepped surface, we will study in detail the diffusion properties of C atoms in Ni subsurface lattice and at the step edges which are closely related to the C segregation process.

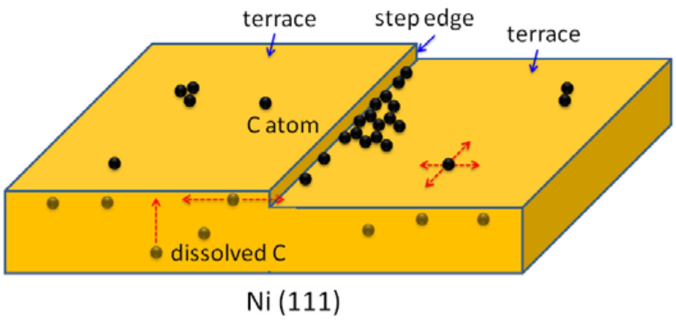

FIG. 1 (color online). A schematic of graphene growth on Ni(111) stepped surface. The growth mode is dominated by the nucleation of the C atoms at the step edges. The arrows indicate the diffusions of the C atoms on the surface and within the Ni lattice.

Ni assumes the face centered cubic atomic structure in which the atoms are 12-coordinated. The (111) surface is close packed as shown in Fig. 2, and the coordination number of the top layer atom is reduced to 9. There are two types of low energy step edges, the A-edge and the B-edge, as shown in the figure too. The atoms in the step edges are 7-coordinated, with the least number of nearest neighbors of the surface atoms. For the atoms in the A-edge, two of the seven nearest neighboring atoms are 12-coordinated and five are less coordinated; For the atoms in the B-edge, only one nearest neighboring atom is 12-coordinated, six are less coordinated.

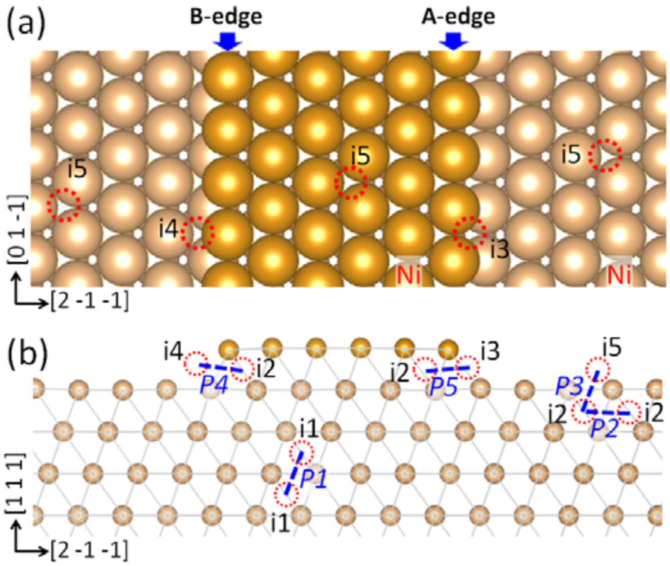

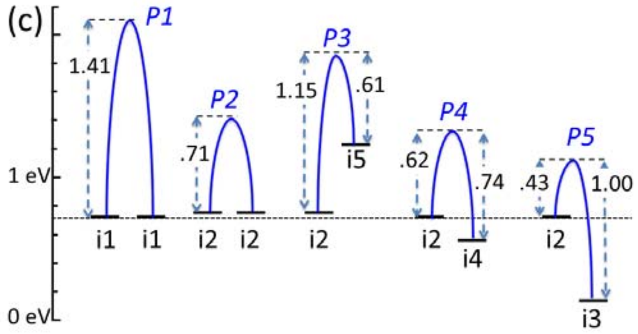

FIG. 2 (color online). (a) The top view and (b) the side view of the two types of step edges on Ni (111) surface in which the brighter orange balls are the atoms in the topmost layer. The dashed circles indicate the locally favorable interstitial sites (i1-i5). The representative diffusion paths (denoted by *P1* to *P5*) of the C atoms are shown in (b). (c) The energy barriers of these diffusion paths. All the interstitial sites in the subsurface are denoted by i2 and all other bulk like sites i1. These sites have very close formation energies respectively.

Using the atomic model shown in Fig. 2, we study the C dissolution at the (111) surface as the start. In bulk Ni, the interstitial C atom (C_i) prefers the octahedral site which connecting the hollow sites in the two adjacent close packed layers. The formation energies of the representative C_is (E_f^Cs) as indicated by Fig. 2 are summarized in Table I. Due to the surface effect, the E_f^C for the C_i at the subsurface i2 site is a little bit increased than the bulk value. On the surface, due to the further reducing of the number of nearest neighbors, the E_f^C (usually called adsorption energy) of the C_i is either increased or decreased. At the B-edge, where the number of the nearest neighbors for the most stable i4 site is reduced to four, the E_f^C is a little bit decreased. At the A-edge where the most stable i3 site has five nearest neighbors, the E_f^C is much decreased. On a hollow site on the terrace, where the number of the nearest neighbors is only three, the E_f^C is the largest, much greater than at any other sites. For all the i1(i2) sites the E_f^Cs are very close. So on the Ni(111) surface, energetically, a C atom prefers to locate at the step edges, especially at the A-edge.

TABLE I The E_f^Cs for the representative sites from i1 to i5 as shown in Fig.2. The values in the brackets are for the Au-alloyed edges under the Au line density of 1/2 as shown in Fig. 4.

Site	i1 (bulk)	i2 (subsurface)	i3 (A-edge)	i4 (B-edge)	i5 (terrace)
Coordination number	6	6	5	4	3
Formation energy (eV)	0.70	0.72	**0.13** (0.88)	0.56 (0.92)	**1.26**

At high temperatures, the kinetic processes like C diffusions become more and more important at the surface. We checked five representative diffusion paths, *P1* to *P5* as shown in Fig. 2(b). The corresponding diffusion barriers (activation energies) are shown in Fig. 2(c). For *P1*, the diffusion from one octahedral site to another within the Ni lattice, the diffusion barrier is as high as 1.41eV. It is also very close to that of an earlier report [28]. For the path *P2*, the diffusion within the subsurface, the barrier is about one half reduced. This is because, during the diffusion, the Ni atoms of the surface layer can relax more substantially than the non-surface atoms due to their less coordinations. Besides, the diffusions along *P1* and *P2* are symmetric, that is, the diffusion barriers don't depend on the directions.

The *P3* represents the diffusion between the surface (site i5) and the subsurface (site i2). The fourth path *P4* is at the B-edge. The fifth path *P5* is at the A-edge. A common feature for the diffusions along these paths is asymmetric. The diffusion barriers depend on the directions.

The above data indicates that, a) it is easier for the C atoms on the terrace to dissolve into the Ni lattice, but more difficult for the dissolved C to get onto the surface again; b) for an C_i in the Ni lattice, the easiest diffusion path is along the subsurface, parallel to the (111) terrace; c) although the A-edge is the most favorable site for the C adsorption, it is not favorable for the adsorbed C to dissolve into the Ni lattice, but the favorable site for the dissolved C to segregate out of the Ni lattice; d) the two types of step edges are contrasting too. So we can see that, for the dissociated C atoms on the Ni(111) surface to dissolve into the lattice, the terrace is the preferred location. To segregate out, the dissolved C atoms will firstly diffuse into the subsurface, then they will diffuse along the subsurface plain until they meet the step edges and, lastly get across the edges onto the surface.

The Ni(111) surface used for the graphene growth is usually not atomic flat and made up of randomly distributed atomic steps. The step edges are more favorable sites for the C accumulation than the terrace, thus the edges become the nucleation centers at the beginning of the growth. The crystalline quality of the grown graphene sheet is closely related to the distribution of the non-correlated step edges that resulted from the surface dynamics as well as kinetics. This is a serious problem for the control of the quality of the grown grapheme sheet. Experimentally high temperatures have to be adopted to improve the uniformity. An alternative is to modify the reactivities of the step edges, and as a consequence the distribution of the nucleation centers, after which the stepped surface becomes uniform for the growth of graphene.

Inspired by the experimental work of Weatherup and coworkers [17], in which the decreased growth temperature and increased structural quality of graphene by a small amount of Au deposited on the surface were reported, we propose that the Au atoms might have altered the chemical properties of the step edges on the Ni(111) surface. As a result, the step edges are no longer the most preferred nucleation centers for the growth of graphene. Although the Ni(111) surface has atomic steps, for the deposited C atoms, it looks like an uniform atomic flat surface, be able to facilitate the large area uniform growth of graphene sheet. Questions need to be further clarified are like, what is the atomic structure of the Au alloyed surface, how the Au atoms on the Ni(111) surface affect the C adsorption and diffusion at the step edges, etc.

We calculate the formation energies (E_f^{Au}s) of substitutional Au atoms (Au_{Ni}) at four representative sites S1-S4 as shown in Fig. 3(a) and the data is summarized in Table II. At the bulk like S1 site, the E_f^{Au} is 0.71 eV. At the terrace site S2, it is -0.43 eV, more than 1 eV reduced compared with at S1 site. This result is also agreeable with an earlier publication of Besenbacher and coworkers [29], in which they claim that the Au atoms prefer to substitute the Ni atoms at the surface rather than in the bulk. The reason is obvious as the authors have pointed out. Because the Au atom has a fully filled d-shell and Ni partially filled, the interaction between Au and Ni is featured by an s-d like interaction, thus Au prefers to locate at the less-coordinated sites like on the surface. This further indicates that the sites in the step edges are even more favored for the Au substitution, because the Ni atoms in the step edges are the least coordinated at the whole surface. Our calculations reveal that the E_f^{Au} at the A-edge is -0.65 eV, at the B-edge is -0.64 eV. The difference between the calculated formation energies at the two types of edges is negligibly small which indicates that the coordination number is the key factor to the interaction between Au and the neighboring Ni atoms. These energies are also the lowest ones for the Au substitution at the whole (111) surface.

The dependence of E_f^{Au} on the density of Au_{Ni}, in terms of line density which is the ratio of the number of Au_{Ni} with the number of original Ni atoms in the edge line, is studied. Three line densities of 1/4, 1/2, and 1 in the A-edge, as the structures shown in Fig. 3, are considered respectively and the calculated E_f^{Au}s are summarized in Table III. We can see that when the density is below 1/2, the E_f^{Au}s are very close, which indicates that the interaction between Au_{Ni}s are weak if they are not nearest neighbors, or to say the effect of Au substitution is well confined within the nearest neighbors. Above 1/2, the E_f^{Au} starts to increase dramatically. At line density of 1, all the Ni atoms in the edge line are replaced by the Au atoms, the E_f^{Au} is increased to -0.33eV, which is even higher than that of an Au_{Ni} at the terrace site (-0.43eV). For the B-edge, the situation is almost identical to the A-edge. Thus we can imagine that with the increase of the amount of Au deposited on the surface, under thermal equilibrium, the Au atoms will substitute the Ni atoms in the step edges firstly. After a critical line density (less than 1), the Au atoms begin to substitute the Ni atoms of the terrace behind the edge lines. It is clear that after the surface alloying of Au, the properties of the step edges on the Ni(111) surface are mostly affected.

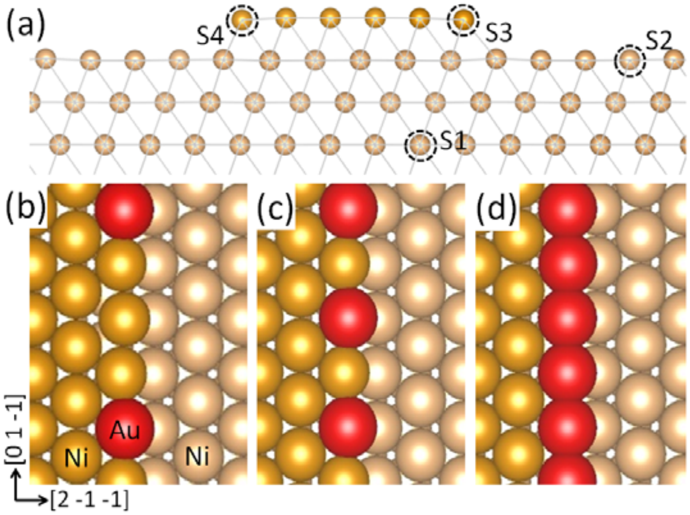

FIG. 3 (color online). (a) Side view of the atomic steps in which the four representative substitutional sites are marked and top views of the atomic structures of the Au alloyed A-edges with Au line densities of (b) 1/4, (c) 1/2, and (d) 1 respectively.

Two properties of the step edges are closely related to the growth of graphene as studied for the clean surface, the formation energy of an adsorbed C atom and the diffusion barriers for the dissolved C to segregate via the step edges. For simplicity, the line density of Au_{Ni} is fixed to ½ for both of the two types of the step edges.

At the Au-alloyed A-edge, the formation energy of an adsorbed C atom (E_f^C) is 0.88eV; at the B-edge, it is 0.92eV as shown in Table I. Compared with the values of 0.13 eV and 0.56 eV for the clean A- and B-edges and of 1.26 eV at the terrace site, the E_f^Cs at the Au-alloyed step edges are much closer to that at the terrace sites. This indicates that the Au-alloying has greatly passivated the active step edges on the Ni(111) surface. For the C atoms deposited on the surface, the step edges are no longer the favorable nucleation centers with strong preference. The chemical differences between the edges and the terrace are greatly reduced after the surface alloying.

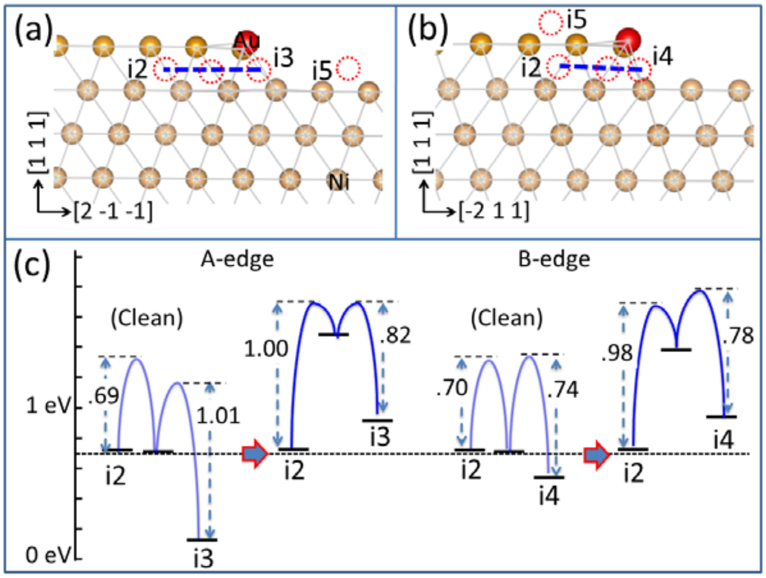

FIG. 4 (color online). The side views of the Au alloyed (a) A-edge and (b) B-edge under the Au line density of 1/2. The favorable segregation processes (diffusion paths) of the dissolved C atom are also shown. (c) The diffusion barriers of the two favorable paths shown in (a) and (b) and of their respective clean edges (in the left) for comparison.

Let's turn to the diffusion properties of the dissolved C atoms at the Au-alloyed step edges. At the A-edge, as shown in Fig. 4(c), the dominating diffusion barrier is ~1.0eV for the C atom to get out of the Ni lattice through the step edge. Compared with the value of 0.69eV for the clean edge, the barrier is increased due to the repelling effect of the Au_{Ni} on the C atom. More importantly, this barrier is closer to that at the Ni (111) terrace site for the dissolved C atom in the subsurface to get out of the Ni lattice (1.15eV). At the B-edge, the dominating barrier is ~0.98eV, very close to the value at the A-edge. So after Au-alloying, the step edges at the Ni (111) surface are also no longer the preferred locations for the C segregation. Therefore, in terms of catalyzing the CVD growth of graphene, on the Au-alloyed Ni (111) surface, the chemical difference between the step edges and the terrace is highly reduced, the surface becomes a much more uniform one compared with the clean surface.

Here we propose a general processing method for the stepped TM surfaces: the surface alloying by other TMs. Usually a clean TM surface is not atomically flat and is made up of atomic steps. The property of the step edges is sharply different from that of the terrace, making the chemical processes on the surface featuring non-uniformity between the terrace and the step edges. This indicates that the opportunity of approaching uniformity of the surface processes resides in tuning the chemical difference between the step edges and the terrace, for which alloying the surface with other TMs can be used. The alloying TM should be able to substitute the atoms only at the step edges, leaving the terraces not affected at all. By choosing different TMs for the alloying and controlling the line density of the substitution, the difference between the edges and the terraces can be modified, providing the ability to optimize the uniformity of the chemical processes on the stepped surface.

TABLE II The formation energies of TM_{Ni} (TM = Au, Ag, Cu, Cd, Zn, Pd, Pt, Co, Fe, and Mn) at the four sites S1-S4 as shown in Fig. 3(a). The numbers of the d-electrons (N_ds) of these TMs are also given. Based on the N_ds, the TMs are divided into two groups with contrasting features of the formation energies.

TM	N_d	Formation Energy (eV)			
		S1 (bulk)	S2 (terrace)	S3 (A-edge)	S4 (B-edge)
Au	10	0.71	-0.43	**-0.65**	**-0.64**
Ag	10	1.28	0.16	**-0.21**	**-0.21**
Cu	10	0.31	-0.02	**-0.17**	**-0.17**
Cd	10	1.09	-0.47	**-0.78**	**-0.80**
Zn	10	-0.31	-0.74	**-0.90**	**-0.92**
Pd	10	0.25	-0.27	**-0.41**	**-0.41**
Pt	9	0.38	-0.01	**-0.03**	**-0.04**
Co	7	**-0.10**	0.05	0.17	0.13
Fe	6	**-0.39**	-0.36	-0.30	-0.30
Mn	5	**-0.38**	-0.27	-0.23	-0.23

In order to find the optimal alloying TMs and the behind mechanism, besides Au, other TMs such as Ag, Cu, Cd, Zn, Pd, Pt, Co Fe, and Mn are also checked for the most preferable substitutional locations on the Ni(111) surface. The data is summarized in Table II. We can see that these TMs are obviously divided into two groups based on the formation energies. The first group includes Au, Ag, Cu, Cd, Zn, Pd, and Pt, of which the N_d is ten or nine, larger than that of Ni (N_d=8). The second group includes Co, Fe and Mn, of which the N_d is less than that of Ni. For the TMs in the first group, the formation energies of the substitutionals at the edge sites are the lowest. On the other hand, for the TMs in the second group, the substitutionals prefer the bulk-like sites. This further confirms that the interaction of the TM substitutionals with the Ni surface depends on the filling of the TM's d-orbitals [29, 30]. The result also indicates that in order to uniform the stepped Ni(111) surface for graphene growth, TMs with N_d larger than that of Ni can only be used.

TABLE III The dependence of the formation energies of Au_{Ni}s at the A-edge on the Au line density.

Line density of Au	1/4	1/2	1
Formation energy (eV)	-0.65	-0.58	-0.33

Similar to the case of Au, the formation energies of the adsorbed C atom (E_f^C) at the alloyed A-edge under the line density of 1/2 for all of these TMs are also calculated. The results are shown in Fig. 5. We see that alloyed with Au corresponds to the largest formation energy whereas with Cu, on the other hand, the lowest for the adsorbed C. The E_f^Cs on other TM-alloyed surfaces are between that of Au and Cu. From the above calculations for the Au-alloyed edge, we understand that the C diffusion barriers at the step edges will follow the similar trend as that of the E_f^Cs at the edges, because they originate from the same interaction between C and the TM_{Ni} [30]. So we can expect the diffusion barriers of the dissolved C at the alloyed edges by these TMs follow the similar trend as shown in Fig. 5(a) for the formation energies. As a result we see that all of these TMs provide varying abilities to tune the catalytic property of the Ni(111) surface for the growth of graphene.

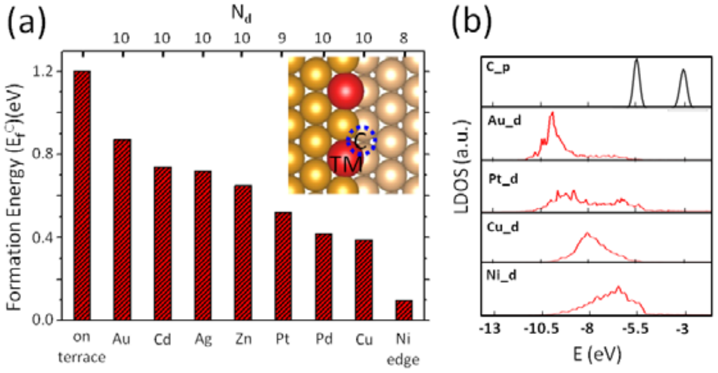

FIG. 5 (color online). (a) The formation energies of the adsorbed C atom at the TM (with N_d larger than that of Ni) alloyed A-edges at line density of ½. The formation energies at the terrace and the clean A-edge are also shown for comparison. In the inset the location of the adsorbed C is shown. (b) The local density of states (LDOSs) of the isolated C atom and the TM_{Ni}s at the A-edge. The LDOSs of the Ni in the A-edge is also shown for comparison. We can see that the formation energy of the adsorbed C is roughly proportional to the energy difference between the mass centers of the C p-orbitals and the TM d-orbitals.

In the experiments, other than catalyzing the growth of graphene, TM surfaces are also widely used in synthesizing other nano materials, like carbon nanotubes and hexangular boron nitride sheets [28, 31]. In nano regime, the surface of the catalyst is made up of terraces with various orientations and the types of atomic step edges are even more abundant. The various types of step edges can play different roles in the growth due to the different chemical reactivities. Whether we can selectively passivate the step edges that play negative roles by surface alloying is attracting. So the general method proposed here potentially has more applications that need to be explored for growing specifically designed structures.

In conclusion, on the Ni (111) surface, the atomic step edges have different properties from the terrace in catalyzing the graphene growth. The step edges are the most preferable sites for C adsorption as well as C segregation from the lattice. Thus the quality of the grown sheet depends highly on the atomic morphology of the surface, like the density of the step edges, the adsorptions at the edges, and also the directions of the edges etc. Alloyed with Au, the Au atoms prefer to substitute the Ni atoms at the step edges, leaving the terraces of the steps unaffected. This will reduce the density of the nucleation centers and make the growth of graphene on the stepped surface more uniform. Other TMs can also be used as the alloying metal but with varying ability in narrowing the difference between the chemical properties of the step edges and the terrace. Here we show how passivating can be used to modify the catalytic property of the TM surfaces.

We acknowledge fruitful discussions with Prof. S.-H. Wei in NREL. The work is supported by the NSF of China with grant Nos. 11074128, 11274179, and 91227101, and National 973 projects of China with Nos. 2011CB922102 and 2012CB921900.

References

[1] K. S. Kim, Y. Zhao, H. Jang, S. Y. Lee. J. M. Kim, K. S. Kim, J.-H. Ahn, P. Kim, J.-Y. Choi, and B. H. Hong, Nature **457**, 706 (2009).

[2] N. Petrone, C. R. Dean, I. Meric, A. M. van der Zande, P. Y. Huang, L. Wang, D. Muller, K. L. Shepard, and J. Hone, Nano Lett. **12**, 2751 (2012).

[3] P. Y. Huang, C. S. Ruiz-Vargas, A. M. van der Zande, W. S. Whitney, M. P. Levendorf, J. W. Kevek, S. Garg, J. S. Alden, C. J. Hustedt, Y. Zhu, J. Park, P. L. McEuen, and D. A. Muller, Nature **469**, 389 (2011).

[4] Q. Yu, L. A. Jauregui, W. Wu, R. Colby, J. Tian, Z. Su, H. Cao, Z. Liu, D. Pandey, D. Wei, T. F. Chung, P. Peng, N. P. Guisinger, E. A. Stach, J. Bao, S.-S. Pei, and Y. P. Chen, Nat. Mater. **10**, 443 (2011).

[5] S. J. Chae, F. Güneş, K. K. Kim, E. S. Kim, E. S. Kim, G. H. Han, S. M. Kim, H.-J. Shin, S.-M. Yoon, J.-Y. Choi, M. H. Park, C. W. Yang, D. Pribat, and Y. H. Lee, Adv. Mater. **21**, 2328 (2009).

[6] G. H. Han, F. Güneş, J. J. Bae, E. S. Kim, S. J. Chae, H.-J. Shin, J.-Y. Choi, D. Pribat, and Y. H. Lee, Nano. Lett. **11**, 4144 (2011).

[7] E. Loginova, N. C. Bartelt, P. J. Feibelman, and K. F. McCarty, New J. Phys. **10**, 093026 (2008).

[8] J. Gao, J. Yip, J. Zhao, B. I. Yakobson, and F. Ding, J. Am. Chem. Soc. **133**, 5009 (2011).

[9] H. Chen, W. Zhu, and Z. Zhang, Phys. Rev. Lett. **104**, 186101 (2010).

[10] J. M. Wofford, S. Nie, K. F. McCarty, N. C. Bartelt, and O. D. Dubon, Nano Lett. **10**, 4890 (2010).

[11] X. Li, C. W. Magnuson, A. Venugopal, R. M. Tromp, J. B. Hannon, E. M. Vogel, L. Colombo, and R. S. Ruoff, J. Am. Chem. Soc. **133**, 2816 (2011).

[12] A. Reina, X. Jia, J. Ho, D. Nezich, H. Son, V. Bulovic, M. S. Dresselhaus, and J. Kong, Nano Lett. **9**, 30 (2009).

[13] X. Li, W. Cai, J. An, S. Kim, J. Nah, D. Yang, R. Piner, A. Velamakanni, I. Jung, E. Tutuc, S. K. Banerjee, L. Colombo, and R. S. Ruoff, Science **324**, 1312 (2009).

[14] W. Moritz, B. Wang, M.-L. Bocquet, T. Brugger, T. Greber, J. Wintterlin, and S. Günther, Phys. Rev. Lett. **104**, 136102 (2010).

[15] P. Lacovig, M. Pozzo, D. Alfè, P. Vilmercati, A. Baraldi, and S. Lizzit, Phys. Rev. Lett. **103**,

166101 (2009).

[16] X. Li, W. Cai, L. Colombo, and R. S. Ruoff, Nano Lett. **9**, 4268 (2009).

[17] R. S. Weatherup, B. C. Bayer, R. Blume, C. Ducati, C. Baehtz, R. Schlögl, and S. Hofmann, Nano Lett. **11**, 4154 (2011).

[18] Y. Zhang, L. Gomez, F. N. Ishikawa, A. Madaria, K. Ryu, C. Wang, A. Badmaev, and C. Zhou, J. Phys. Chem. Lett. **1**, 3101 (2010).

[19] R. Addou, A. Dahal, P. Sutter, and M. Batzill, Appl. Phys. Lett. **100**, 021601 (2012).

[20] R. S. Weatherup, B. Dlubak, and S. Hofmann, ACS Nano **6**, 9996 (2012).

[21] Y. Cho, Y. C. Choi, and K. S. Kim, J. Phys. Chem. C **115**, 6019 (2011).

[22] S. Bae, H. Kim, Y. Lee, X. Xu, J.-S. Park, Y. Zheng, J. Balakrishnan, T. Lei, H. R. Kim, Y. I. Song, K. S. Kim, B. Özyilmaz, J.-H. Ahn, B. H. Hong and S. Iijima, Nat. Nanotechnol. **5**, 574 (2010).

[23] G. Kresse and J. Hafner, Phys. Rev. B **47**, 558 (1993); Phys. Rev. B **49**, 14251 (1994).

[24] J. P. Perdew, K. Burke, and M. Ernzerhof, Phys. Rev. Lett. **77**, 3865 (1996).

[25] A.V. Chichagov, Kristallographiya **35**, 610 (1990).

[26] M. Fuentes-Cabrera, M. I. Baskes, A. V. Melechko, and M. L. Simpson, Phys. Rev. B **77**, 035405 (2008).

[27] G. Mills, H. Jónsson, and G. K. Schenter, Surf. Sci. **324**, 305 (1995).

[28] S. Hofmann, G. Csányi, A. C. Ferrari, M. C. Payne, and J. Robertson, Phys. Rev. Lett. **95**, 036101 (2005).

[29] F. Besenbacher, I. Chorkendorff, B. S. Clausen, B. Hammer, A. M. Molenbroek, J. K. Nørskov, and I. Stensgaard, Science **279**, 1913 (1998).

[30] B. Hammer and J. K. Nørskov, Adv. Catal. **45**, 71(2000).

[31] P. Sutter, J. Lahiri, P. Albrecht, and E. Sutter, ACS Nano **5**, 7303 (2011).